

Research

Differential curcumin absorption and curcumin-induced STAT3 inhibition during 3T3-L1 cell adipogenesis in 2D and 3D cultures

Sehee Yang¹ · Soyeon Lee¹ · Youngjoo Kwon¹

Received: 19 September 2023 / Accepted: 4 January 2024

Published online: 20 January 2024

© The Author(s) 2024 [OPEN](#)

Abstract

It is increasingly considered that 3D cell culture systems are superior to 2D in evaluating health promoting effects of candidate molecules because they better mimic tissue-like structures, thus testing in such systems will increase their *in vivo* applicability. The present study sought to examine the potential usefulness of spheroid models for assessing the antiadipogenic effect of polyphenols. The major food polyphenols were compared for their antiadipogenic effects in 3T3-L1 cells grown in conventional 2D conditions and as 3D spheroids. Further, the study evaluated the effect of the cell culture environment on the inhibition of the adipogenesis-related signaling pathway mediated by curcumin (CUR), the most effective antiadipogenic polyphenol identified in 2D and 3D, and its cellular absorption rate. CUR treatment inhibited the activity of signal transducer and activator of transcription 3 (STAT3) in cells cultured in both conditions; however, it was more effective in 2D. Notably, 3T3-L1 preadipocytes in a 3D cell culture system maintained high STAT3 activity and CCAAT/enhancer-binding protein alpha (C/EBP α) expression compared with a 2D system. Additionally, the cellular absorption rate was lower in 3D cultures. Thus, different cellular absorption rates, innate STAT3 activity, and C/EBP α expression levels may contribute to the difference in CUR efficacy. This study demonstrated that the STAT3 inhibition at least partly contributes to antiadipogenic effect of CUR. Moreover, it showed that the presentation of cells in 3D significantly alters activation of intracellular signaling pathways and absorption rate of CUR. Therefore, 3D spheroid models are valuable tools to evaluate the anti-adipogenicity of candidate molecules.

Highlights

- Curcumin inhibits STAT3 activity on adipogenesis induction in 2D and 3D cell cultures; however, the inhibition is less in the 3D culture.
- Culturing 3T3-L1 preadipocytes in 3D cell cultures maintained a high STAT3 activity and C/EBP α expression levels compared with 2D systems.
- Curcumin's cellular absorption rate was lower in the 3D compared with the 2D cell culture, although repeated treatments increased both the cellular absorption and efficacy.

Keywords 3T3-L1 adipocyte · Adipogenesis signaling · Cellular absorption · Curcumin · Polyphenol · Spheroid

✉ Youngjoo Kwon, Youngjoo.Kwon@ewha.ac.kr; Sehee Yang, yangse0504@naver.com; Soyeon Lee, soy1011chel@gmail.com |
¹Department of Food Science and Biotechnology, Ewha Womans University, 52 Ewhayeodae-gil, Seodaemun-gu, Seoul 03760, Republic of Korea.



1 Introduction

Obesity is rising rapidly and has become a major public health concern worldwide [1]. Furthermore, obesity is a common cause of low-grade systemic inflammation, which greatly contributes to increased risk of various diseases, including coronary heart disease, hypertension, type 2 diabetes mellitus, osteoarthritis, and cancer [2]. Adipose tissue mass increases via the hypertrophy of mature adipocytes and the differentiation of preadipocytes into new adipocytes in a process known as adipogenesis [3]. Adipocyte differentiation is regulated by genetic and environmental factors, and its inhibition may serve as an effective therapeutic intervention in preventing obesity [4]. In light of this, various food-derived compounds have been studied, and polyphenols have shown great promise [3, 5, 6].

Two-dimensional (2D) cell culture techniques have been exclusively used to evaluate antiadipogenic effects of polyphenols. However, 2D *in vitro* systems may not reflect the complex three-dimensional (3D) *in vivo* environment in which cells are exposed to concentration gradients of oxygen, nutrients, and cellular metabolites due to cell–cell and cell–matrix interactions in all directions [7]. Thus, 3D cell culture systems better represent *in vivo* conditions [7, 8]. Particularly, spheroid cell cultures have been useful due to their simplicity and reproducibility [9]. Multicellular spheroids show greater structural and functional resemblance to living tissues than 2D monolayer cell cultures [7, 9, 10]. Notably, cells in spheroids exhibit different characteristics from monolayer cells in terms of transcriptome profile [9] and drug response [11, 12]. Therefore, 3D cell culture systems can represent certain aspects of cell behaviors *in vivo* and provide important information when used in combination with 2D cell culture techniques.

Spheroid models of adipocytes, including 3T3-L1 cells, have been addressed [7, 9], however, they have not yet been used to evaluate antiadipogenic molecules, including polyphenols, on preadipocyte differentiation. Polyphenol absorption through multicellular layers can be relatively more challenging, a factor that could contribute to differences in their efficacy in cells grown in 3D compared with 2D cell culture conditions. Additionally, 3D cell culture conditions alter the intrinsic activity of different cellular signaling pathways, *i.e.*, decrease in AKT activity and increase in extracellular signal-regulated kinase (ERK) and signal transducer and activator of transcription 3 (STAT3) activities [13–15], which may also affect the anti-adipogenicity of polyphenols.

This study examined the usefulness of 3T3-L1 spheroids for identification and evaluation of potential antiadipogenic molecules such as polyphenols. The major polyphenol compounds found in plant foods were compared for their antiadipogenic effect in 3T3-L1 cells grown in conventional 2D conditions and as 3D spheroids. Further, the study evaluated the effect of the cell culture environment on the inhibition of the adipogenesis-related signaling pathways mediated by curcumin (CUR), the most effective anti-adipogenic polyphenol identified, and its cellular absorption rate.

2 Materials and methods

2.1 Polyphenols

All plant polyphenols, apigenin (API; $\geq 95\%$), CUR ($\geq 80\%$), chlorogenic acid (CHL; $\geq 95\%$), epigallocatechin gallate (EGCG; $\geq 80\%$), quercetin (QUE; $\geq 95\%$), and resveratrol (RES; $\geq 99\%$) were purchased from Sigma-Aldrich Inc. (St. Louis, MO, USA). Polyphenol compounds were dissolved in dimethyl sulfoxide (DMSO) as a 100 mM stock solution and then diluted to final concentrations using cell culture media. The final concentration of DMSO was less than 0.04%.

2.2 3T3-L1 cell culture

Mouse preadipocyte 3T3-L1 cells were purchased from the American Type Culture Collection (Manassas, VA, USA) and maintained in Dulbecco's modified Eagle's medium (DMEM) supplemented with 10% calf serum. Cells were cultured in a humidified incubator at 37 °C and 5% CO₂. All reagents were purchased from Thermo Fisher Scientific, Inc. (Waltham, MA, USA).

2.3 Adipocyte differentiation in 2D and 3D cell cultures

The 3T3-L1 cells (20,000 cells/mL) were plated in a 24-well plate for the 2D culture. The differentiation was initiated 2 days after the cells reached 100% confluence by replacing the media with MDI media (DMEM containing 10% fetal bovine serum [FBS] supplemented with 3-isobutyl-1-methylxanthine, dexamethasone, and insulin to final concentrations of 0.5 mM, 1 μ M, and 10 μ g/mL, respectively). After 3 days, the MDI media was replaced with insulin media (DMEM containing 10% FBS and 10 μ g/mL of insulin). After 3 days, the insulin media was replaced with DMEM containing 10% FBS, and cultured for 3 days to complete differentiation.

For the spheroid culture, 3T3-L1 cells (750,000 cells/mL) were deposited in 20 μ L drops onto the bottom of a lid. Afterward, the lid was inverted and placed on a phosphate-buffered saline (PBS)-filled bottom chamber. Two days later, cell aggregates were transferred to a 96-well ultra-low attachment plate, and differentiation was initiated by changing the media as described in the 2D cell culture. The 3T3-L1 spheroids were imaged using an EVOS M5000 imaging system (Thermo Fisher Scientific) to monitor their size increase. The size of spheroids was estimated by measuring the area of three individual spheroids for each treatment using ImageJ (National Institutes of Health, Bethesda, MD, USA). After completion of differentiation, spheroids were washed with PBS and fixed in 10% formalin for 2 h. The fixed spheroids were embedded in 4% agarose, cut into 4 μ m sections, and placed onto slides for hematoxylin and eosin staining. Polyphenols or vehicle control (CON) were treated in MDI media once unless otherwise specified.

2.4 Oil-Red-O staining

The differentiated 3T3-L1 cells were fixed with 10% formalin and washed. The cells were then rinsed with 60% isopropanol for 1 min, followed by incubation with a freshly prepared Oil-Red-O (ORO) working solution for 20 min. After washing the cells three times with water, images were obtained using an EVOS M5000 imaging system. The red staining was then extracted from the fixed cells with 100% isopropanol, and their absorbance was determined at 492 nm using a VersaMax ELISA microplate reader (Molecular Devices, Sunnyvale, CA, USA).

2.5 Cell viability assay

The 3T3-L1 preadipocytes (40,000 cells/well) were cultured in maintenance media in 96-well plates overnight to attach. Subsequently, the cells were incubated with polyphenols or CON for 72 h. Afterward, 3-[4,5-dimethylthiazol-2-yl]-2,5 diphenyl tetrazolium bromide (MTT) (BioVision, Inc., Milpitas, CA, USA) was added, and the plates were incubated for a further 4 h. The cell viability was determined by measuring absorbance at 540 nm using a VersaMax ELISA microplate reader.

2.6 Immunoblotting

Proteins were extracted using radio-immunoprecipitation assay buffer supplemented with a protease inhibitor cocktail and a mixture of sodium orthovanadate, sodium fluoride, and β -glycerophosphate (Sigma-Aldrich). Afterward, cell debris was removed by centrifugation at 13,000 rpm for 10 min, and the resulting supernatants were stored at -80°C until analysis. The protein concentration was determined using a protein assay kit (Bio-rad Laboratories, Inc., Hercules, CA, USA). For immunoblotting, the protein samples (50 μ g) were denatured and separated by 10% sodium dodecyl-sulfate polyacrylamide gel electrophoresis (SDS-PAGE). Target proteins were conjugated with the indicated primary antibodies, followed by the secondary antibodies (Cell Signaling Technology, Inc., Danvers, MA, USA). Primary antibodies against CCAAT/enhancer-binding protein alpha (C/EBP α), peroxisome proliferator-activated receptor gamma (PPAR γ), phospho-STAT3, phospho-AKT, phospho-ERK, phospho-insulin-like growth factor 1 receptor (IGF1R), ERK, AKT, and tubulin were purchased from Cell Signaling Technology and STAT3 was purchased from Santa Cruz Biotechnology, Inc. (Dallas, TX, USA). The proteins were detected using a SuperSignal West Pico Plus (Thermo Fisher Scientific).

2.7 Leptin enzyme-linked immunosorbent assay

Media derived from the differentiated adipocytes were collected to measure the secreted leptin levels after the completion of 3T3-L1 preadipocyte differentiation. The collected media were centrifuged at 13,000 rpm for 10 min, and the obtained supernatants were frozen at -80°C until analysis. Leptin levels were measured using a leptin Elisa kit (Ray Biotech Life, Inc., Norcross, GA, USA) according to the manufacturer's instructions.

2.8 Triacylglycerol level

After completion of adipocyte differentiation, spheroids were washed with PBS and lysed using 5% NP-40. Spheroid lysates were subjected to two cycles of heating ($80\text{--}100^{\circ}\text{C}$) and cooling. Afterward, cell debris was removed by centrifugation at 13,000 rpm for 2 min, and the remaining supernatants were stored at -80°C until analysis. The triacylglycerol (TAG) concentration was measured by the detection of a colorimetric product (absorbance at 540 nm) of oxidized glycerol following the conversion of TAG to free fatty acids and glycerol using a Triglyceride Quantification Kit (BioVision) according to the manufacturer's instructions.

2.9 High-performance liquid chromatography analysis

The 3T3-L1 preadipocytes cultured in 2D and 3D environments were treated with various concentrations of CUR ($0\text{--}40\ \mu\text{M}$) for different times ($0\text{--}24\ \text{h}$). For the repeated CUR treatments, the cells were initially treated for 3 days from the start of differentiation, followed by treatments every 2 days over 5 days. Then, the cells were extracted 2 h after the final treatment. On the day of extraction, cells were also singly treated for 2 h before the extraction to estimate the CUR levels attached or absorbed to the cell surface. The CUR levels in the media and cells were measured using a previous HPLC method with slight modification as described below [16].

The CUR was extracted from the media using the same volume of 4% acetic acid dissolved in 100% acetonitrile (ACN). The media extracts were centrifuged at 13,000 rpm for 15 min, and the resulting supernatants were stored at -20°C until analysis. To determine the cellular level of CUR, the cells were lysed using 0.5% Triton after washing thoroughly three times with PBS. Then, cell lysates were mixed with an equal volume of 4% acetic acid dissolved in 100% ACN and sonicated for 1 min. The cell extracts were centrifuged at 13,000 rpm for 15 min, and the resulting supernatants were collected and stored at -20°C until analysis. All the samples were filtered into an HPLC sample vial through a $0.2\ \mu\text{m}$ syringe filter for HPLC analysis.

A Gilson HPLC system (Gilson, Inc., Middleton, WI, USA) equipped with an auto-injector and an ultraviolet-visible detector set at 425 nm was used for the HPLC analysis. The CUR was separated using a Zorbax 300SB-C18 ($4.6 \times 250\ \text{mm}$, $5\ \mu\text{m}$) column (Agilent Technologies, Inc., Santa Clara, CA, USA) by elution with isocratic ACN/2% acetic acid (40/60, v/v) with a 1 mL/min flow rate. The injection volume was 20 μL . The CUR standard was dissolved in the eluent at various concentrations (1.84, 3.68, 7.37, and 14.7 $\mu\text{g}/\text{mL}$) and analyzed under the same analytical conditions as the samples. The obtained standard curves (peak area against concentration) were used to quantify the CUR levels in the media ($\mu\text{g}/\text{mL}$) and cells ($\mu\text{g}/\text{mg}$) after normalization to protein concentration.

For the recovery test, CUR (1.84, 3.68, and 7.36 $\mu\text{g}/\text{mL}$) was spiked into the media and cells, and the recovery rates were determined ($79.6 \pm 5.1\%$, $81.9 \pm 5.4\%$, and $91.4 \pm 3.4\%$, respectively in the media; $100.2 \pm 5.3\%$, $120.2 \pm 3.3\%$, and $114.6 \pm 9.0\%$, respectively in the cells). There was high linearity between the CUR concentration and peak area, with a correlation coefficient of 0.9998. The limit of detection and limit of quantification (LOQ) were 0.31 and 0.93 $\mu\text{g}/\text{mL}$, respectively. All the solvents used in the preparation of the solutions, extraction, and analysis were of analytical or HPLC grade.

2.10 Statistical analyses

Statistical analyses were conducted using SAS software (version 9.4; SAS Institute, Inc., Cary, NC, USA), and p-values less than 0.05 were considered significant and indicated as follows: *** for $p < 0.001$, ** for $p < 0.01$, and * for $p < 0.05$. The student's *t*-test was used to examine the differences between the CON and each polyphenol treatment group. In addition, student's *t*-test was performed for the following comparisons: CON and CUR treatment at different time

points, and single and repeated treatments of CUR on its absorption at the cellular level. Two-way analysis of variance (ANOVA) was used to examine the main effect of repeated CUR treatments on antiadipogenic activity.

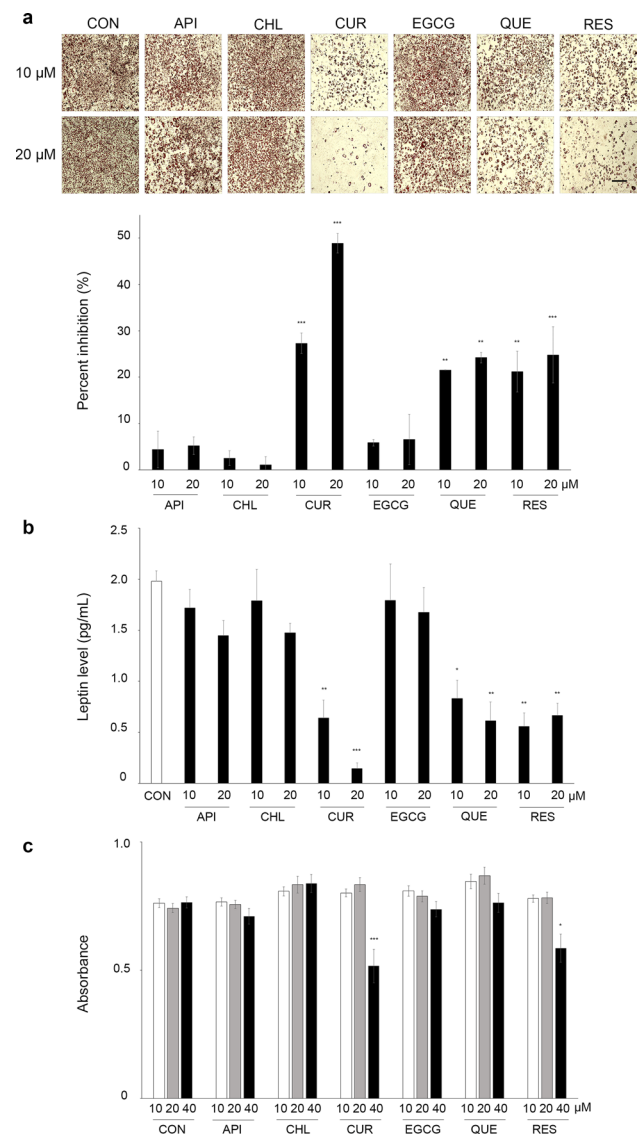
3 Results

3.1 Inhibitory effect of polyphenols on adipocyte differentiation in 2D cell cultures

The 3T3-L1 cells were differentiated into adipocytes in the presence of various polyphenols during the first 3 d of differentiation to compare their antiadipogenic efficacy. Treatments of CUR, QUE, and RES inhibited the differentiation of preadipocytes into mature adipocytes; this was evident from the significantly lower fat (ORO staining) accumulation (Fig. 1a). The dose-dependent effect was most apparent with 10 and 20 μM CUR, at 27% and 49% inhibition, respectively, compared with vehicle-treated control (CON). In comparison, the treatment with 10 and 20 μM of QUE inhibited adipocyte differentiation by 17% and 24%, respectively, and 10 and 20 μM of RES by 20% and 24%, respectively. Treatment with API, CHL, or EGCG did not inhibit adipogenesis (Fig. 1a).

Adipocytes secrete leptin, and its level can reflect fat mass [17, 18]. Similar to the results of ORO staining, leptin levels derived from the differentiated 3T3-L1 adipocytes were significantly decreased after treatment with CUR, QUE, and RES; however, CUR was the most effective (Fig. 1b). The leptin level of the CON was 1.98 pg/mL, which decreased to 0.64 and

Fig. 1 Effect of polyphenols on 3T3-L1 adipogenesis in 2D cell culture conditions. The effect of apigenin (API), chlorogenic acid (CHL), curcumin (CUR), epigallocatechin gallate (EGCG), quercetin (QUE), and resveratrol (RES) at 10 and 20 μM concentrations for 3 days at the start of differentiation on fat accumulation was estimated using Oil-Red-O (ORO) staining and secreted leptin level. **a** Representative images of differentiated adipocytes stained with ORO (upper panel) and percentage inhibition of fat accumulation (absorbance of ORO extract at 490 nm) relative to vehicle-treated control (CON) (lower panel). Scale bar; 200 μm . **b** Levels of leptin secreted from differentiated adipocytes. **c** Cytotoxicity of polyphenols was assessed using a 3-[4,5-dimethylthiazol-2-yl]-2,5 diphenyl tetrazolium bromide (MTT) assay. Optical density values are shown. Values: mean \pm SE; $n = 3$; * $p < 0.05$, ** $p < 0.01$, and *** $p < 0.001$, compared with the CON



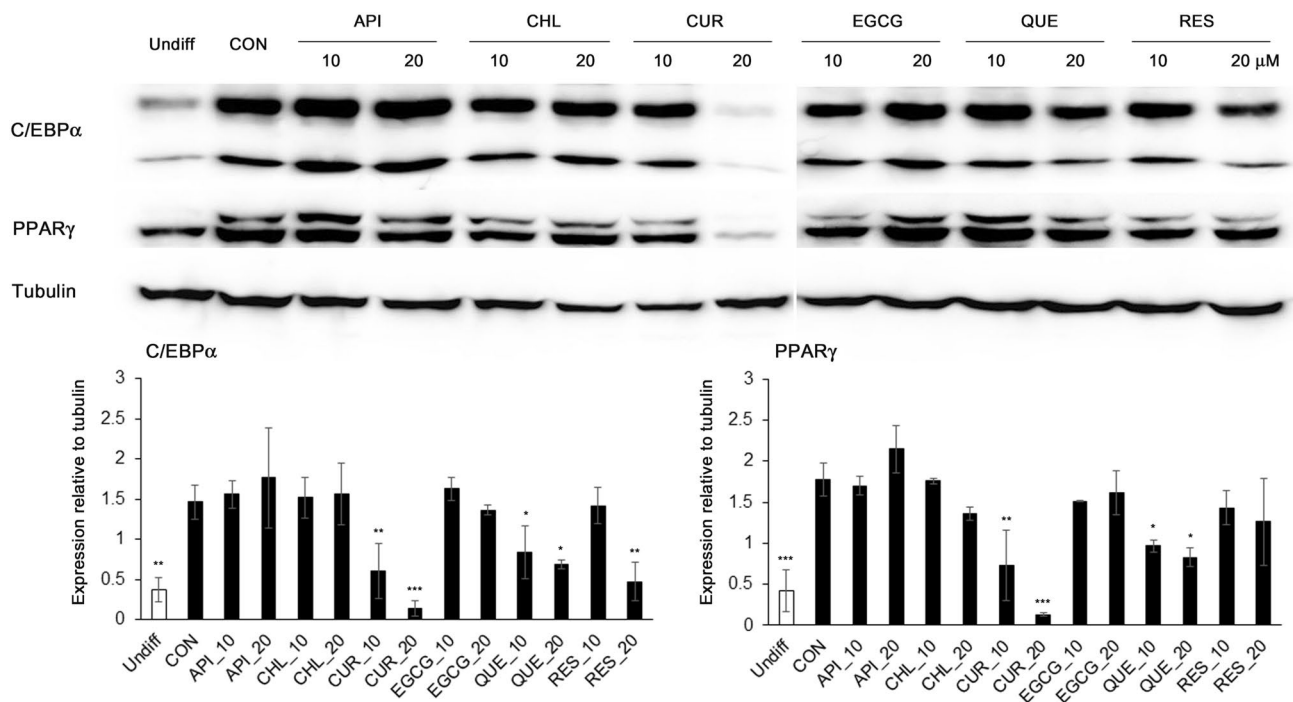


Fig. 2 Effect of polyphenols on the expression levels of adipose differentiation-related proteins. The 3T3-L1 cells were extracted after 48 h incubation with various polyphenols (apigenin [API], chlorogenic acid [CHL], curcumin [CUR], epigallocatechin gallate [EGCG], quercetin [QUE], and resveratrol [RES]) at 10 and 20 μM on starting differentiation or left undifferentiated (Undiff). Representative western blot images are shown in the upper panel. Densitometric analysis is shown in the lower panel. Values: mean \pm SE; $n=3$; * $p < 0.05$, ** $p < 0.01$, and *** $p < 0.001$, compared with the vehicle-treated control (CON)

0.15 pg/mL following treatments with 10 and 20 μM of CUR, respectively. There was a less apparent decrease after 10 and 20 μM of QUE (0.83 and 0.61 pg/mL, respectively) and RES (0.56 and 0.67 pg/mL, respectively). In contrast, leptin levels were not significantly different compared with the CON for API, CHL, and EGCG treatments (Fig. 1b). The observed inhibitory effect of CUR, QUE, and RES on adipogenesis may not be due to cytotoxicity as cell viability was not affected at 10 and 20 μM treatments of all polyphenols tested (Fig. 1c). However, at 40 μM , CUR and RES significantly decreased the 3T3-L1 cell viability.

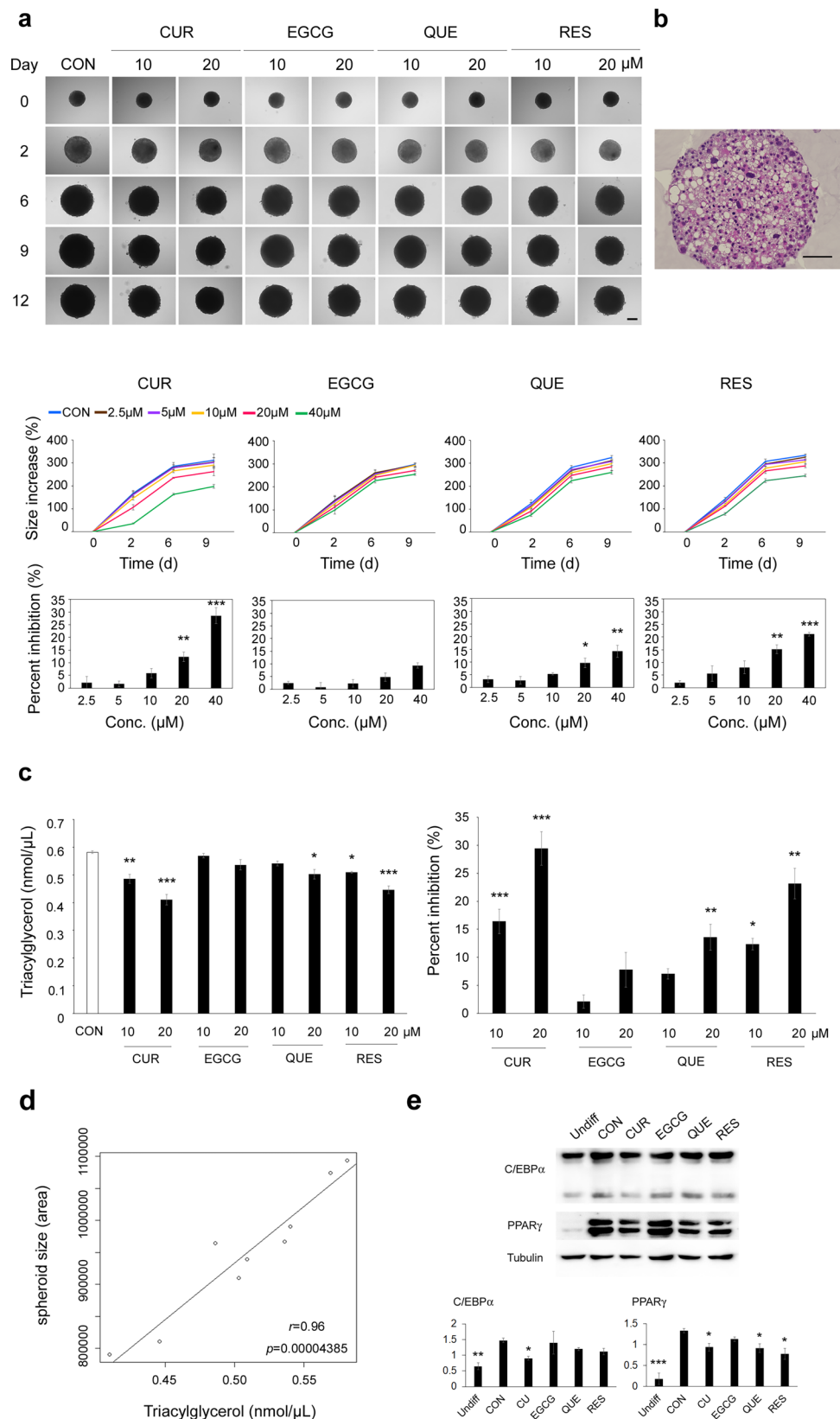
Polyphenols treatments made similar effect on the expression of major adipogenic transcription factors. Treatment with 10 or 20 μM of CUR markedly inhibited the expression of PPAR γ and C/EBP α levels increased upon differentiation (Fig. 2). Treatment with QUE at 10 and 20 μM and RES at 20 μM also resulted in a significant decrease in the expression of C/EBP α , although less so compared with CUR treatment. Additionally, treatment with QUE at 10 and 20 μM significantly inhibited the increase in PPAR γ expression (Fig. 2). At the same concentrations, API, CHL, and EGCG did not significantly alter the expression of PPAR γ or C/EBP α .

3.2 Inhibitory effect of polyphenols on adipocyte differentiation in 3D cell cultures

The 3T3-L1 spheroid model was used to examine whether the antiadipogenic effects of polyphenols observed in 2D cell culture conditions were retained in 3D environments. The 3T3-L1 cells were induced to differentiate into spheroids and treated with various concentrations of CUR, EGCG, QUE, or RES for 3 d following inducing the adipocyte differentiation to determine the concentration that requires for comparable antiadipogenic effect observed in 2D. Spheroids increased in size during differentiation; the undifferentiated preadipocytes increased their diameter from approximately 300 to 800 μm over the 12-day culture period (Fig. 3a). Fat accumulation was apparent in spheroids differentiated for 8 d (Fig. 3b). Notably, the spheroids contained mostly unilocular lipid droplets (Fig. 3b), which is characteristic of complete adipocyte differentiation [8].

Treatments with CUR, QUE, and RES significantly inhibited the increase in the 3T3-L1 spheroid size compared with CON (Fig. 3a). At 10, 20, and 40 μM of CUR treatment, the spheroid sizes were inhibited by 8%, 14%, and 30%, respectively, compared with the CON. In comparison, the inhibition was reduced by half to two-thirds following treatment

Fig. 3 Effect of polyphenols on 3T3-L1 adipogenesis in 3D cell culture conditions. The 3T3-L1 cells were induced to differentiate in spheroids, and curcumin (CUR), epigallocatechin gallate (EGCG), quercetin (QUE), and resveratrol (RES) were treated for 3 days upon induction of differentiation at various concentrations. **a** Representative images of the 3T3-L1 spheroids during differentiation (0–9 days). Scale bar; 200 μ m. **b** A representative image of a hematoxylin and eosin-stained spheroid section. Scale bar; 100 μ m. **c** Triacylglycerol (TAG) levels in the left panel and percentage inhibition compared with the vehicle-treated control (CON) in the right panel. **d** Correlation between spheroid size and TAG level. **e** Representative western blot images are shown in the upper panel. Densitometric analysis is shown in the lower panel. Values: mean \pm SE; $n=3$; * $p < 0.05$, ** $p < 0.01$, and *** $p < 0.001$, compared with the CON



with the same concentrations (10, 20, and 40 μM) of QUE (5%, 10%, and 14%, respectively) and RES (6%, 13%, and 21%, respectively; Fig. 3b). However, treatment with EGCG did not significantly inhibit spheroid growth even at the highest concentration (Fig. 3b). Similarly, triacylglycerol (TAG) accumulation was significantly reduced after treatment with CUR, QUE, or RES compared with the CON (Fig. 3c). The TAG content in the CON was 0.58 nmol/ μL ; treatment with 10 and 20 μM CUR decreased the TAG content by 16% and 29%, respectively (Fig. 3c). In comparison, the 10 and 20 μM QUE treatments inhibited the TAG accumulation by 7% and 14%, respectively compared with the CON. At 10 and 20 μM of RES treatment, the TAG accumulation was inhibited by 12% and 23%, respectively (Fig. 3c). Spheroid size and TAG content showed a significant positive correlation ($r=0.96$, $p=4.385\text{e}-05$) (Fig. 3d). As the spheroid size increased (or cells became more differentiated), the TAG content increased, although the TAG level may be a more sensitive method to assess the antiadipogenic efficacy of polyphenols than the spheroid size (Fig. 3a, c). As in 2D cell cultures, the increase of protein expression levels of C/EBP α and PPAR γ were effectively inhibited in 3T3-L1 spheroids by 20 μM CUR (Fig. 3e). Treatment with same concentration of QUE and RES also decreased the expression levels of both proteins; however, a significant decrease only occurred in PPAR γ levels (Fig. 3e). Collectively, the results demonstrated that CUR was the most effective polyphenol in the 3D cell culture environment. However, antiadipogenic effect of CUR was lower in 3D compared with 2D cell culture conditions.

3.3 Effect of CUR treatment on adipogenesis-induced cellular signaling activation in 2D and 3D cell cultures

Multiple signaling pathways, including AKT, IGF1R, STAT3, and ERK pathways, are involved in the early stage of adipogenesis differentiation [19–23]. These signaling pathways can also be activated by cell–cell and cell–extracellular matrix (ECM) interactions. Cells grown as 3D spheroids have different cell–cell and cell–ECM interactions compared with cells cultivated in a 2D culture environment. Therefore, 3D spheroids may potentiate different cellular signaling pathways. Moreover, this difference in their innate ability to activate adipogenesis-related signaling pathways may affect CUR-induced antiadipogenic activity. Treatment with CUR had apparent antiadipogenic effect at 20 μM in both 2D and 3D conditions. Thus, 20 μM CUR was used to examine the effect of culture condition and CUR treatment on the activation of adipogenicity-related signaling pathway.

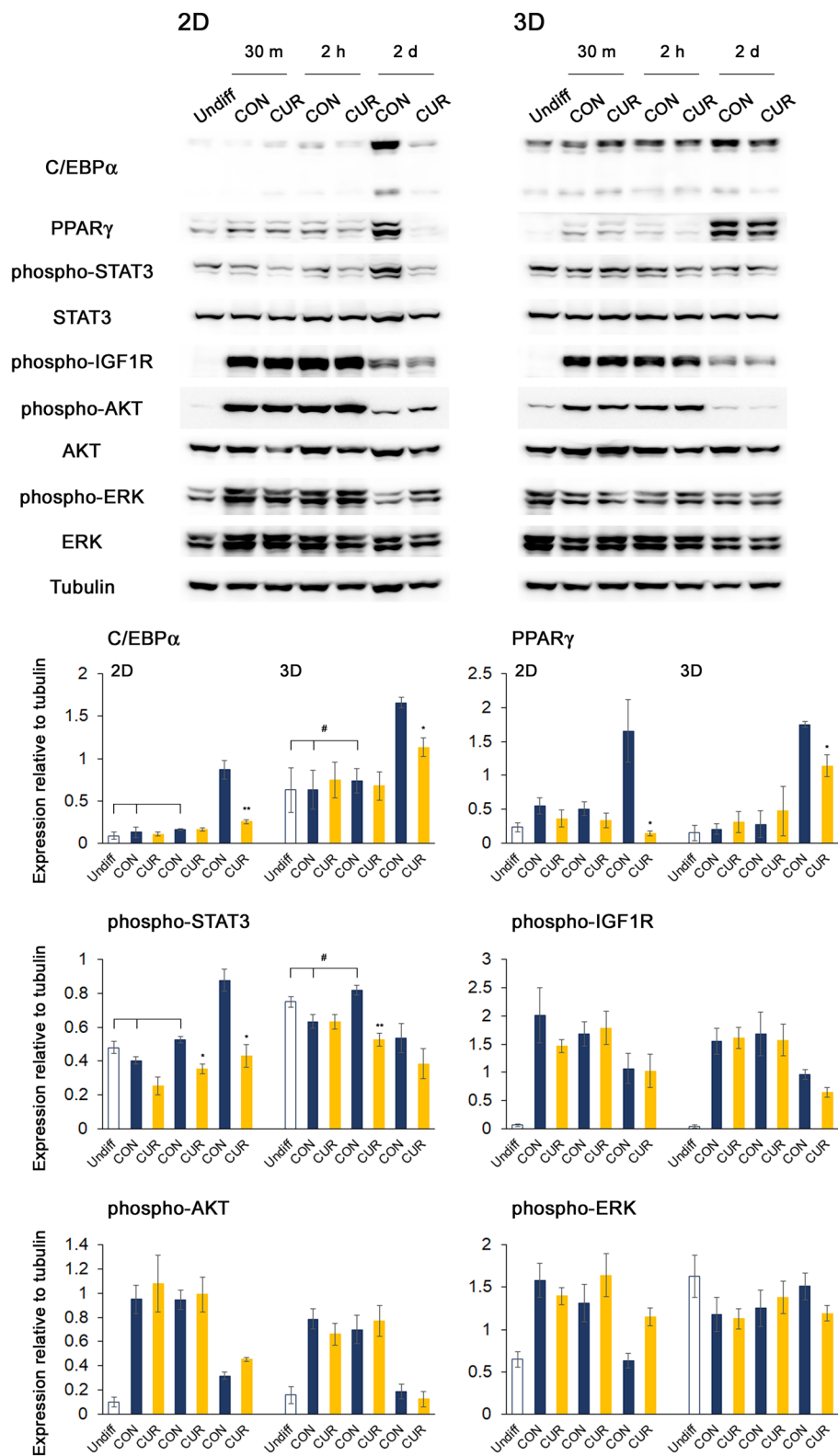
Consistently, inhibitory effects of CUR on C/EBP α and PPAR γ expressions were reduced in the 3D compared with the 2D (Fig. 4). The culturing environment greatly influenced the activities of ERK and STAT3 at an undifferentiated state and upon adipogenic induction. In an undifferentiated state, activities of ERK and STAT3 were greater in the 3T3-L1 preadipocytes cultured in the 3D compared with the 2D condition. Particularly, at the beginning of adipogenesis (0–2 h), cells in 3D exhibited higher STAT3 activation and C/EBP α expression compared with cells in the 2D environment (Fig. 4). However, when 3T3-L1 preadipocytes were differentiated, they were reduced or similar to undifferentiated state in 3D, whereas they were markedly increased in 2D conditions although the required time was different (Fig. 4).

Culturing 3T3-L1 cells in 3D conditions also altered the activation of other adipogenesis-related signaling pathways during differentiation. For example, culturing 3T3-L1 cells in a 2D environment highly and acutely increased the expression levels of phospho-AKT and phospho-IGF1R (Fig. 4). AKT and IGF1R activation also occurred soon after inducing adipogenesis in cells cultured in a 3D environment, as observed in 2D; however, the extent of activation was much reduced. Thus, the activation of AKT, IGF1R, STAT3, and ERK signaling pathways in response to adipogenic stimulus was substantially different between 3D and 2D cell cultures. This difference may also affect the efficacy of CUR. The CUR treatment effectively inhibited STAT3 activation at 2 h following inducing differentiation in both cell culture environments. However, inhibitory effect of CUR on STAT3 activity was reduced at 2 d of differentiation in 3D environments in contrast to apparent inhibition in 2D conditions (Fig. 4). CUR treatment did not significantly alter other adipogenesis-related signaling pathways, including IGF1R, AKT, and ERK (Fig. 4).

3.4 Cellular absorption of CUR in 2D and 3D cell cultures

The anti-adipogenic effect of CUR was greater in 2D than 3D cell cultures. It was examined whether this difference is also related to the cellular absorption rate of CUR. The addition of 5, 10, 20, and 40 μM CUR resulted in 0.39, 1.09, 2.48, 5.56, and 12.63 $\mu\text{g}/\text{mL}$ of CUR in the 2D cell culture media, respectively, and the levels gradually decreased with time for all concentrations (Fig. 5a). Notably, a large amount of CUR was bound to the cell surfaces and was detected even after extensive cell washing immediately after the treatment (0 h); consequently, 0.95, 3.02, and 5.69 $\mu\text{g}/\text{mg}$ of protein was detected at 10, 20, and 40 μM , respectively. At the cellular level, the CUR concentration reached the highest level at 2 h after the treatment. The detected values were 0.49, 1.83, and 2.71 $\mu\text{g}/\text{mg}$ of protein after 10, 20,

Fig. 4 Effect of the cell culture environment and curcumin (CUR) on the activation of adipogenesis-relating signaling pathways. **a** The 3T3-L1 cells were treated with 20 μ M CUR or left undifferentiated (Undiff) while they were differentiated in 2D or 3D culture conditions, and the effect of the cell culture environment and CUR treatment on the activation of adipogenesis-related signaling pathway was evaluated by immunoblotting. Representative western blot images are shown in the upper panel. Densitometric analysis is shown in the lower panel. Values: mean \pm SE; $n=3$; * $p < 0.05$ and ** $p < 0.01$, compared with the vehicle-treated control (CON). #Indicates a significant difference ($p < 0.05$) between the 2D and 3D culture environments using a two-way analysis of variance



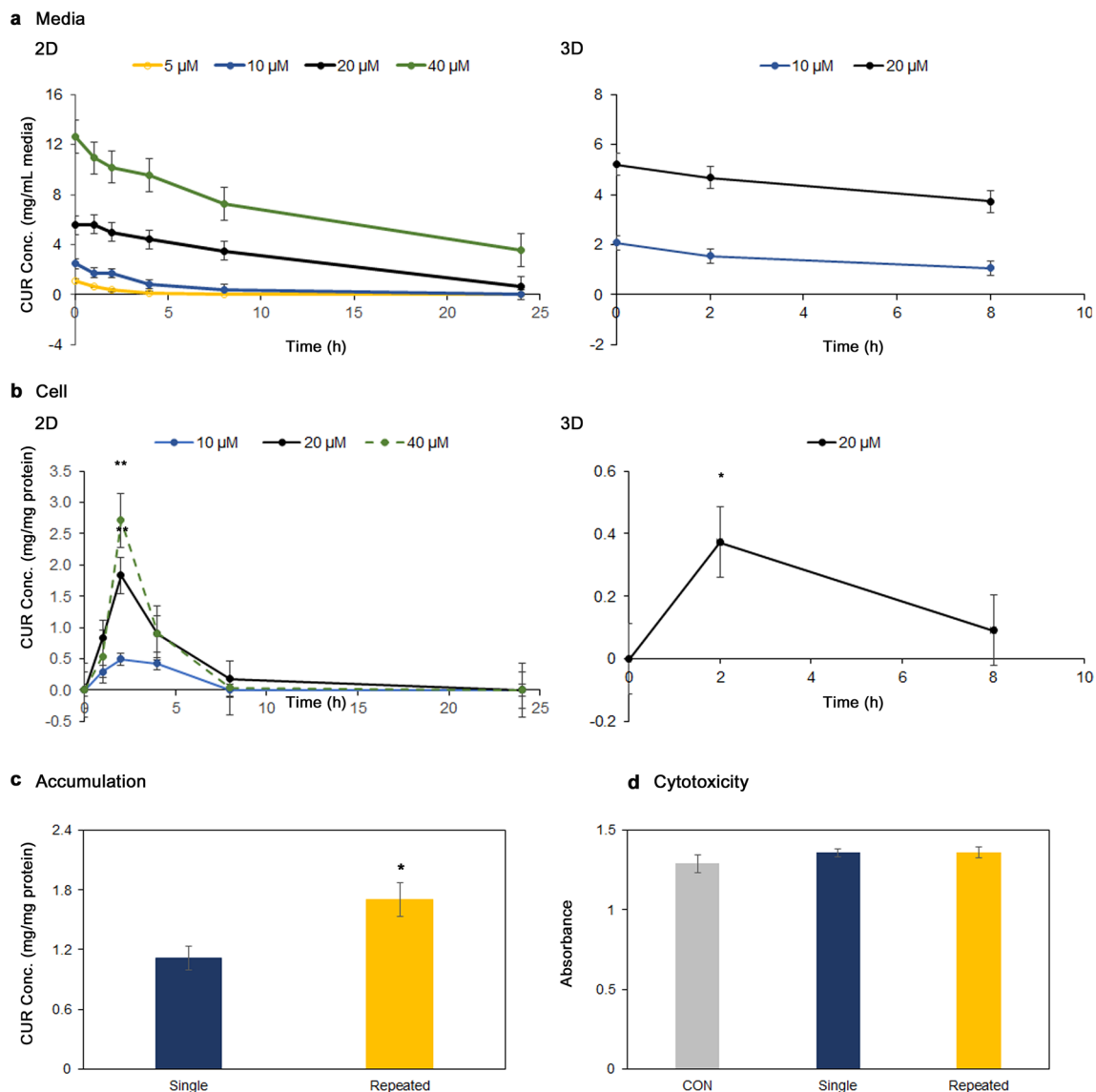


Fig. 5 Curcumin (CUR) levels in the culture media and 3T3-L1 cells in the 2D and 3D environments. The CUR was added to the culture media in the 2D and 3D systems, and its levels in the media and 3T3-L1 cells were monitored over time. **a** The CUR levels in the media in 2D (left) and 3D (right) cultures. **b** The CUR levels in the 3T3-L1 cell cultured in 2D monolayer (left) and spheroids (right). Cellular levels were derived by subtracting the CUR level at 0 h from levels obtained at each time point. **c** The cellular CUR levels of a single treatment and repeated treatments. The CUR levels were measured 2 h after the final treatment at 5 days after the start of 3T3-L1 differentiation in 2D cell culture conditions. **d** Cytotoxicity of polyphenols was assessed using a 3-[4,5-dimethylthiazol-2-yl]-2,5 diphenyl tetrazolium bromide (MTT) assay. Optical density values are shown. Values: mean \pm SE; $n=3$; * $p < 0.05$ and ** $p < 0.01$, compared with 0 h or single treatment

and 40 μM of CUR treatments, respectively, when subtracting the levels at 0 h (Fig. 5b); this corresponded to 15%, 16%, and 11% CUR absorption, respectively, by the cells (2 h) from the media (0 h). The cellular level of CUR rapidly decreased after 2 h; no detectable level remained 24 h after the treatment (Fig. 5b). The addition of 5 μM of CUR led to levels below the LOQ.

In spheroid cultures, the CUR levels in the media were 2.07 and 5.20 $\mu\text{g}/\text{mL}$ with 10 and 20 μM treatments, respectively, similar to the levels in the 2D cell cultures (Fig. 5a). The CUR levels in the spheroid were also significantly higher 2 h after the treatment compared with 0 h (Fig. 5b). However, the spheroid CUR levels were much lower compared with cells grown in 2D environments, reaching only 0.37 $\mu\text{g}/\text{mg}$ of protein after treatment with 20 μM of CUR. The cellular CUR level was under the LOQ following a 10 μM treatment. Therefore, only 5% of the CUR was absorbed into the spheroids from the media, approximately one-third of the cellular absorption observed in the 2D cell cultures. The levels of CUR attached to the cell surface were much lower in the spheroids, 0.15 $\mu\text{g}/\text{mg}$ with a 20 μM CUR treatment, corresponding to only

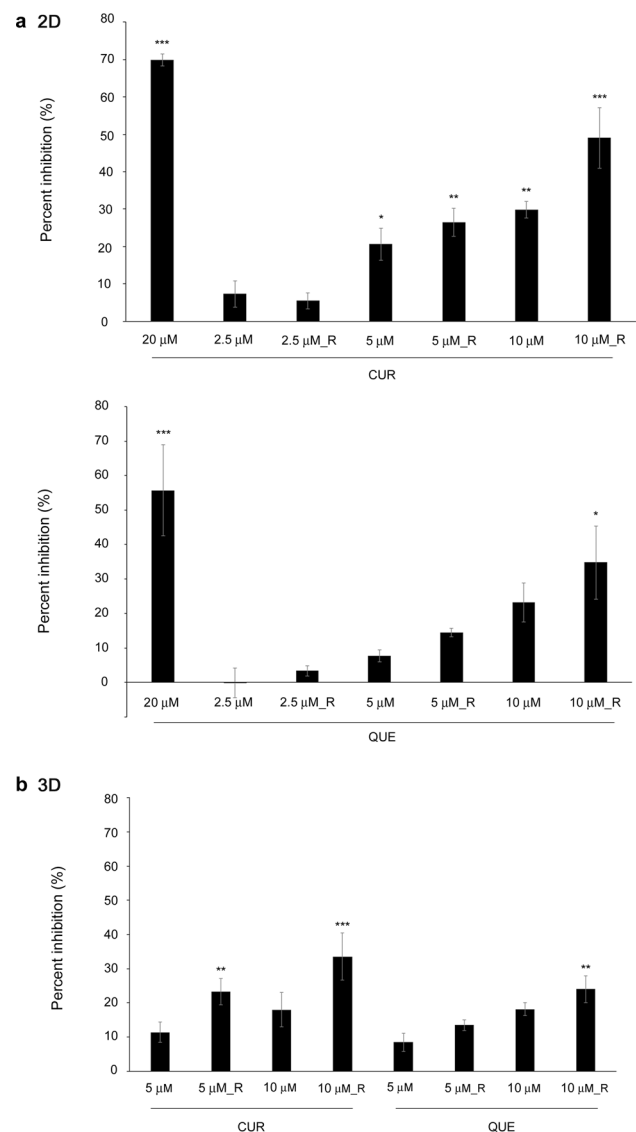
5% of the 2D cell culture levels. These results may be because more extensive washing (in all directions) is achievable in spheroids, and fewer cells are directly in contact with the media compared with 2D systems.

Cellular CUR absorption rate was very low. To determine whether cellular CUR can be accumulated by repeated treatments, a 10 μM of CUR treatment was repeated (at 3 and 5 days after the start of differentiation), and cellular absorption levels were compared with single treatment in the 2D cell cultures. The CUR levels increased by repeated treatment, resulting in 1.71 $\mu\text{g}/\text{mg}$ of protein compared with 1.11 $\mu\text{g}/\text{mg}$ of protein at a single treatment, which resulted in a significant difference between the single and a repeated treatment (Fig. 5c). Repeated treatments with 10 μM CUR did not appreciably affect cell viability compared with a single treatment (Fig. 5d). Thus, observed increase in CUR absorption may not be due to preferential attachment of CUR onto the dead cells.

3.5 Effect of repeated CUR and QUE treatments on antiadipogenicity in the 2D and 3D cell cultures

Repeated low-dose exposure may be more physiologically relevant. Moreover, cellular CUR level increased after repeated treatments. Thus, the CUR treatment was repeated for 11 d (treated alternate days after the initial 3-day treatment, total 5 times) to test whether repeated treatments with low doses could enhance its antiadipogenic effect compared with a single treatment (initial 3-day treatment). Repeated CUR treatments did not induce cytotoxicity (Fig. 5d). However, the repeated treatments increased CUR's antiadipogenic effect in both the 2D ($p=0.0393$) and 3D ($p=0.0236$) cell cultures, based on two-way ANOVA for treatments with 5 and 10 μM of CUR (Fig. 6a, b). Repeated treatments of 10 μM of CUR

Fig. 6 Effect of repeated curcumin (CUR) or quercetin (QUE) treatments on 3T3-L1 cell adipogenesis. The CUR or QUE were singly (initial 3-day treatment after starting differentiation) or repeatedly treated (2.5 μM_R , 5 μM_R and 10 μM_R) for 11 days (alternate days after the initial 3-day treatment). **a** The 3T3-L1 cells were differentiated in 2D culture conditions, and fat accumulation was estimated using Oil-Red-O (ORO) staining. The percentage fat accumulation inhibition (absorbance of ORO extract at 490 nm) relative to the vehicle-treated control (CON). **b** The 3T3-L1 cells were differentiated into spheroids and cellular triacylglycerol (TAG) levels were measured. The percentage of TAG level inhibition is reported compared with the CON. Values: mean \pm SE; $n=3$; * $p < 0.05$, ** $p < 0.01$, and *** $p < 0.001$, compared with the CON



enhanced the inhibition of lipid accumulation by over 1.6-fold compared with a single treatment in the 2D cell culture system (30% vs. 49% inhibition) and by 1.8-fold in the 3D conditions (18% vs. 34% inhibition). Repeated treatments with QUE also increased the antiadipogenic effect compared with a single treatment, but this was only apparent at 10 μM (Fig. 6a).

4 Discussion

The inhibition of adipogenesis is an effective strategy for managing obesity. 3T3-L1 preadipocyte 2D cell culture systems have been extensively used to evaluate anti-adipogenicity. However, 3D cell culture environments, which resemble better *in vivo* conditions, may alter antiadipogenic effect of polyphenols due to potential differences in cellular absorption and activation of cellular signaling pathways in cells presented in 3D compared with 2D conditions.

Previous studies evaluated the antiadipogenic effects of polyphenols using 2D cell cultures at relatively high concentrations (20–100 μM) [6, 24–27], thus low bioavailability of polyphenols was not fully considered [28]. In the current study, CUR exhibited the most effective antiadipogenic effect in 2D conditions (Figs. 1 and 2). QUE and RES also inhibited the adipogenesis of 3T3-L1 cells but had a comparatively lower inhibitory effect (Figs. 1 and 2). API, CHL, and EGCG may require a higher concentrations and prolonged exposure compared with CUR, QUE, and RES to effectively inhibit adipogenesis of 3T3-L1 preadipocytes. Importantly, antiadipogenic effect of CUR was retained in the 3D spheroid culture conditions (Figs. 3 and 4). However, the CUR efficacy was lower in 3D compared with 2D culture conditions.

Culturing cells in spheroids has been shown to alter the basal and induced activation of cellular signaling pathways, probably due to different cell–cell and cell–ECM interactions in 3D compared with 2D environments [13, 29]. For example, cell–cell adhesion is mediated by cadherins, and this engagement can trigger the activation of STAT3 [30]. In contrast, integrin-mediated adhesion that anchor cells to the underlying ECM (or the plastic surface) can cause activation of focal adhesion kinase, which in turn activates the AKT pathway [12, 15, 30]. Figure 4 shows that the 3T3-L1 cells presented in 3D cultures enhanced basal activation of the STAT3 and ERK pathways as have been demonstrated previously [12, 13, 29, 31]. Cells being differentiated in 3D environments also had the reduced ability to activate AKT, IGF1, and ERK in response to adipogenic stimuli (Fig. 4). Thus, culturing 3T3-L1 cells in 3D conditions altered basal and adipogenesis-induced activation of signaling pathways compared with cells presented in 2D conditions. Coincidentally, higher phospho-STAT3 expression occurred together with the higher expression of C/EBP α in the 3D compared with the 2D cell culture at undifferentiated preadipocytes and early stages of differentiation into adipocytes (Fig. 4). The relationship of high STAT3 activity with increased C/EBP α expression needs to be further evaluated in the future. Interestingly, STAT3 activation augmented the transcription level and activity of C/EBP α during granulocyte colony-stimulating factor-induced granulocyte differentiation [32]. Therefore, presentation of 3T3-L1 cells in 3D environments may induce differential activation of signaling pathways and expression of transcription factors related with adipogenesis compared with culturing cells in 2D environments.

The differential signaling activation capabilities in cells cultured in the 3D may contribute to the lower efficacy of CUR. In comparison to no effects of CUR treatment on activation of IGF1R, AKT, and ERK, it effectively reduced STAT3 activity in both culture conditions, suggesting that CUR may exert the antiadipogenic effect through inhibiting STAT3 signaling pathway. However, inhibitory effect of CUR on phospho-STAT3 expression was reduced in 3D environments in contrast to marked inhibition in 2D environments particularly at the later time (2 d) of differentiation (Fig. 4). Activation of STAT3 may be required to maintain multicellular structures of 3D spheroids [29, 31], making it difficult to inhibit. Thus, higher intrinsic STAT3 activity in cells presented in 3D may lead to the lower efficacy of CUR. This finding suggested that antiadipogenic molecules possessing an ability to inhibit STAT3 possibly reduce their effect in 3D compared with 2D environments. Additionally, the lower efficacy of CUR in 3D compared with 2D cell cultures is likely related to the lower cellular absorption of CUR in 3D spheroids (Fig. 5b). Nevertheless, CUR can cross the cell membrane due to its lipophilicity. Repeated CUR treatments increased the cellular CUR levels (Fig. 5c), probably contributing to its improved efficacy in 2D and 3D conditions (Fig. 6).

5 Conclusion

It is increasingly important to consider 3D cell culture systems, which mimic tissue-like structures better. Moreover, the presentation of cells in 3D cell cultures can significantly alter the ability to activate adipogenesis-related signaling pathways and the absorption rate of substances into the cell. Of the polyphenols tested, CUR was the most effective

antiadipogenic in 2D and 3D cell culture conditions, and thus this study results support CUR as a promising candidate in preventing and managing obesity. However, CUR treatments were less effective when 3T3-L1 cells were differentiated in a 3D, which may be attributed to high intrinsic activity of STAT3 and CEBP α and lower cellular CUR absorption when cells were presented in 3D cell cultures. Therefore, 3D spheroid models are valuable together with 2D cell cultures to evaluate the anti-adipogenicity of polyphenols and enhance their in vivo applicability.

Acknowledgements This work was supported by the National Research Foundation of Korea under Grant 2017R1D1A1B03034185 and the Ottogi Foundation under Grant 16-241 to YK.

Author contributions SY and SL carried out experiments, prepared the figures, and analyzed the data; YK conceived the work, carried out experiments, analyzed the data, and wrote the manuscript.

Data availability The datasets used and analyzed during the current study are available from the corresponding author on reasonable request.

Declarations

Competing interests The authors declare no competing interests.

Open Access This article is licensed under a Creative Commons Attribution 4.0 International License, which permits use, sharing, adaptation, distribution and reproduction in any medium or format, as long as you give appropriate credit to the original author(s) and the source, provide a link to the Creative Commons licence, and indicate if changes were made. The images or other third party material in this article are included in the article's Creative Commons licence, unless indicated otherwise in a credit line to the material. If material is not included in the article's Creative Commons licence and your intended use is not permitted by statutory regulation or exceeds the permitted use, you will need to obtain permission directly from the copyright holder. To view a copy of this licence, visit <http://creativecommons.org/licenses/by/4.0/>.

References

1. WHO. Obesity and overweight. 2020 9 June 2021. <https://www.who.int/news-room/fact-sheets/detail/obesity-and-overweight>. Accessed 16 June 2023.
2. Kwon Y. Immuno-resolving ability of resolvin, protectin, and maresin derived from Omega-3 fatty acids in metabolic syndrome. *Mol Nutr Food Res*. 2020;64:e1900824. <https://doi.org/10.1002/mnfr.201900824>.
3. Jakab J, Miskic B, Miksic S, Juranic B, Cosic V, Schwarz D, Vcev A. Adipogenesis as a potential anti-obesity target: a review of pharmacological treatment and natural products. *Diabetes Metab Syndr Obes*. 2021;14:67–83. <https://doi.org/10.2147/Dmso.S281186>.
4. Haider N, Larose L. Harnessing adipogenesis to prevent obesity. *Adipocyte*. 2019;8:98–104. <https://doi.org/10.1080/21623945.2019.1583037>.
5. Hithamani G, Ganesan P. Polyphenols from Indian cereal grains inhibit 3T3-L1 adipogenesis through modulating early and late phase adipogenic markers. *Food Biosci*. 2022;50:102075. <https://doi.org/10.1016/j.fbio.2022.102075>.
6. Kim CY, Le TT, Chen CY, Cheng JX, Kim KH. Curcumin inhibits adipocyte differentiation through modulation of mitotic clonal expansion. *J Nutr Biochem*. 2011;22:910–20. <https://doi.org/10.1016/j.jnutbio.2010.08.003>.
7. Klingelhutz AJ, Gourronc FA, Chaly A, Wadkins DA, Burand AJ, Markan KR, Idiga SO, Wu M, Potthoff MJ, Ankrum JA. Scaffold-free generation of uniform adipose spheroids for metabolism research and drug discovery. *Sci Rep*. 2018;8:523. <https://doi.org/10.1038/s41598-017-19024-z>.
8. Baganha F, Schipper R, Hagberg CE. Towards better models for studying human adipocytes. *Adipocyte*. 2022;11:413–9. <https://doi.org/10.1080/21623945.2022.2104514>.
9. Turner PA, Garrett MR, Didion SP, Janorkar AV. Spheroid culture system confers differentiated transcriptome profile and functional advantage to 3T3-L1 adipocytes. *Ann Biomed Eng*. 2018;46:772–87. <https://doi.org/10.1007/s10439-018-1993-y>.
10. Duval K, Grover H, Han LH, Mou Y, Pegoraro AF, Fredberg J, Chen Z. Modeling physiological events in 2D vs. 3D cell culture. *Physiology (Bethesda)*. 2017;32:266–77. <https://doi.org/10.1152/physiol.00036.2016>.
11. Melissaridou S, Wiechec E, Magan M, Jain MV, Chung MK, Farnebo L, Roberg K. The effect of 2D and 3D cell cultures on treatment response, EMT profile and stem cell features in head and neck cancer. *Cancer Cell Int*. 2019;19:16. <https://doi.org/10.1186/s12935-019-0733-1>.
12. Riedl A, Schleder M, Pudelko K, Stadler M, Walter S, Unterleuthner D, Unger C, Kramer N, Hengstschlager M, Kenner L, Pfeiffer D, Krupitza G, Dolznig H. Comparison of cancer cells in 2D vs 3D culture reveals differences in AKT-mTOR-S6K signaling and drug responses. *J Cell Sci*. 2017;130:203–18. <https://doi.org/10.1242/jcs.188102>.
13. Damianova R, Stefanova N, Cukierman E, Momchilova A, Pankov R. Three-dimensional matrix induces sustained activation of ERK1/2 via Src/Ras/Raf signaling pathway. *Cell Biol Int*. 2008;32:229–34. <https://doi.org/10.1016/j.cellbi.2007.08.029>.
14. Gangadhara S, Smith C, Barrett-Lee P, Hiscox S. 3D culture of Her2+ breast cancer cells promotes AKT to MAPK switching and a loss of therapeutic response. *BMC Cancer*. 2016;16:345. <https://doi.org/10.1186/s12885-016-2377-z>.
15. Geletu M, Adan H, Niit M, Arulanandam R, Carefoot E, Hoskin V, Sina D, Elliott B, Gunning P, Raptis L. Modulation of Akt vs Stat3 activity by the focal adhesion kinase in non-neoplastic mouse fibroblasts. *Exp Cell Res*. 2021;404:112601. <https://doi.org/10.1016/j.yexcr.2021.112601>.

16. Setyaningsih D, Santoso YA, Hartini YS, Murti YB, Hinrichs WLJ, Patramurti C. Isocratic high-performance liquid chromatography (HPLC) for simultaneous quantification of curcumin and piperine in a microparticle formulation containing *Curcuma longa* and *Piper nigrum*. *Heliyon*. 2021;7:e06541. <https://doi.org/10.1016/j.heliyon.2021.e06541>.
17. Chihara K, Hattori N, Ichikawa N, Matsuda T, Saito T. Re-evaluation of serum leptin and adiponectin concentrations normalized by body fat mass in patients with rheumatoid arthritis. *Sci Rep*. 2020;10:15932. <https://doi.org/10.1038/s41598-020-73068-2>.
18. Picó C, Palou M, Pomar CA, Rodríguez AM, Palou A. Leptin as a key regulator of the adipose organ. *Rev Endocr Metab Dis*. 2022;23:13–30. <https://doi.org/10.1007/s11154-021-09687-5>.
19. Al Dow M, Silveira MAD, Poliquin A, Tribouillard L, Fournier E, Trebaol E, Secco B, Villot R, Tremblay F, Bilodeau S, Laplante M. Control of adipogenic commitment by a STAT3-VSTM2A axis. *Am J Physiol Endocrinol Metab*. 2021;320:E259–69. <https://doi.org/10.1152/ajpendo.00314.2020>.
20. Jo MJ, Kim SJ, Go HJ, Park NG, Kim GD. Anti-adipogenic effects of α AL14 mediated by modulation of PI3K/Akt pathways in 3T3-L1 cells. *Int J Pept Res Ther*. 2021;27:1913–22. <https://doi.org/10.1007/s10989-021-10220-0>.
21. Li N, Chen K, Dong HW, Yang J, Yoshizawa M, Kagami H, Li XQ. Alliin inhibits adipocyte differentiation by downregulating Akt expression: Implications for metabolic disease. *Exp Ther Med*. 2021;21:563. <https://doi.org/10.3892/etm.2021.9995>.
22. Yuan YY, Xi Y, Chen JY, Zhu P, Kang JY, Zou ZQ, Wang FY, Bu SZ. STAT3 stimulates adipogenic stem cell proliferation and cooperates with HMGA2 during the early stage of differentiation to promote adipogenesis. *Biochem Biophys Res Commun*. 2017;482:1360–6. <https://doi.org/10.1016/j.bbrc.2016.12.042>.
23. Wang C, Li XM, Dang HX, Liu P, Zhang B, Xu F. Insulin-like growth factor 2 regulates the proliferation and differentiation of rat adipose-derived stromal cells via IGF-1R and IR. *Cytotherapy*. 2019;21:619–30. <https://doi.org/10.1016/j.jcyt.2018.11.010>.
24. Ahn J, Lee H, Kim S, Ha T. Curcumin-induced suppression of adipogenic differentiation is accompanied by activation of Wnt/beta-catenin signaling. *Am J Physiol-Cell Physiol*. 2010;298:C1510–6. <https://doi.org/10.1152/ajpcell.00369.2009>.
25. Tian L, Song Z, Shao W, Du WW, Zhao LR, Zeng K, Yang BB, Jin T. Curcumin represses mouse 3T3-L1 cell adipogenic differentiation via inhibiting mir-17-5p and stimulating the wnt signalling pathway effector Tcf7l2. *Cell Death Dis*. 2017;8:e2559. <https://doi.org/10.1038/cddis.2016.455>.
26. Rayalam S, Yang JY, Ambati S, Della-Fera MA, Baile CA. Resveratrol induces apoptosis and inhibits adipogenesis in 3T3-L1 adipocytes. *Phytother Res*. 2008;22:1367–71. <https://doi.org/10.1002/ptr.2503>.
27. Yang JY, Della-Fera MA, Rayalam S, Ambati S, Hartzell DL, Park HJ, Baile CA. Enhanced inhibition of adipogenesis and induction of apoptosis in 3T3-L1 adipocytes with combinations of resveratrol and quercetin. *Life Sci*. 2008;82:1032–9. <https://doi.org/10.1016/j.lfs.2008.03.003>.
28. Hu Y, Lin QZ, Zhao H, Li XJ, Sang SY, McClements DJ, Long J, Jin ZY, Wang JP, Qiu C. Bioaccessibility and bioavailability of phytochemicals: influencing factors, improvements, and evaluations. *Food Hydrocoll*. 2023;135:108165. <https://doi.org/10.1016/j.foodhyd.2022.108165>.
29. Edsbacker E, Serviss JT, Kolosenko I, Palm-Apergi C, De Milito A, Tamm KP. STAT3 is activated in multicellular spheroids of colon carcinoma cells and mediates expression of IRF9 and interferon stimulated genes. *Sci Rep*. 2019;9:536. <https://doi.org/10.1038/s41598-018-37294-z>.
30. Niit M, Hoskin V, Carefoot E, Geletu M, Arulanandam R, Elliott B, Raptis L. Cell–cell and cell–matrix adhesion in survival and metastasis: Stat3 versus Akt. *Biomol Concepts*. 2015;6:383–99. <https://doi.org/10.1515/bmc-2015-0022>.
31. Huang YH, Molavi O, Alshareef A, Haque M, Wang Q, Chu MP, Venner CP, Sandhu I, Peters AC, Lavasanifar A, Lai R. Constitutive activation of STAT3 in myeloma cells cultured in a three-dimensional, reconstructed bone marrow model. *Cancers*. 2018;10:206. <https://doi.org/10.3390/cancers10060206>.
32. Numata A, Shimoda K, Kamezaki K, Haro T, Kakumitsu H, Shide K, Kato K, Miyamoto T, Yamashita Y, Oshima Y, Nakajima H, Iwama A, Aoki K, Takase K, Gondo H, Mano H, Harada M. Signal transducers and activators of transcription 3 augments the transcriptional activity of CCAAT/enhancer-binding protein alpha in granulocyte colony-stimulating factor signaling pathway. *J Biol Chem*. 2005;280:12621–9. <https://doi.org/10.1074/jbc.M408442200>.

Publisher's Note Springer Nature remains neutral with regard to jurisdictional claims in published maps and institutional affiliations.